Isoselective Styrene Polymerization Catalyzed by ansa-Bis(indenyl) Allyl Rare Earth Complexes. Stereochemical and Mechanistic Aspects

ARTICLE *in* MACROMOLECULES · APRIL 2011

Impact Factor: 5.8 · DOI: 10.1021/ma2003757

Macromolecules

ARTICLE

pubs.acs.org/Macromolecules

Isoselective Styrene Polymerization Catalyzed by *ansa*-Bis(indenyl) Allyl Rare Earth Complexes. Stereochemical and Mechanistic Aspects

Liana Annunziata,[†] Anne-Sophie Rodrigues,[†] Evgeny Kirillov,[†] Yann Sarazin,[†] Jun Okuda,[‡] Lionel Perrin,[§] Laurent Maron,[§] and Jean-François Carpentier*[,†]

[†]Sciences Chimiques de Rennes, UMR 6226, CNRS-Université de Rennes 1, F-35042 Rennes Cedex, France

[‡]Institute of Inorganic Chemistry, RWTH Aachen University, Landoltweg 1, D-52056 Aachen, Germany

[§]LPCNO, UMR 5215, Université de Toulouse-CNRS, INSA, UPS, 135 avenue de Rangueil, F-31077 Toulouse Cedex 4, France

Supporting Information

ABSTRACT: Mechanistic features of the isoselective polymerization of styrene promoted by *racemic* allyl *ansa*-lanthanidocene complexes *rac*-{$CMe_2(Ind)_2$}Ln(allyl)$(THF)_n$ (Ind =5-indenyl; allyl = C_3H_5, n = 1, Ln = Y (**1**), Nd (**2**); allyl =1,3-$(SiMe_3)_2C_3H_3$, n = 0, Ln = Y (**3**), Nd (**4**)), which act as unique single-component catalysts, have been investigated by experimental and theoretical methods. Combined ^{1}H NMR and MALDI−ToF−MS analyses conducted on low molecular weights isotactic polystyrene (iPS) produced by compounds **1** or **2** established the presence of allyl end-groups and therefore that polymerization is initiated by insertion of styrene into Ln−C(allyl). ^{1}H, ^{2}D, and ^{13}C NMR analyses performed on H(D)-iPS-*n*Bu polymers, selectively produced by coordinative chain transfer polymerization (CCTP) of styrene with the binary system **3**/Mg(*n*Bu)$_2$ (1:10), evidenced that the polymerization is highly regioselective and proceeds in a secondary insertion mode, both in the initiation and propagation steps. Microstructural analyses of the backbone of *crude* (unfractionated) polymers produced with **1**−**4** evidenced a virtually perfect isoselective (*mmmmmm* > 0.99) polymerization up to 120 °C. Stereoerrors observed in the ^{13}C{^{1}H} NMR spectra of the iPS produced at 130 °C with **1**−**4** are consistent with an enantiomorphic site control operative during the polymerization. DFT computations of the first and second insertions of styrene in **3** confirmed the above features and the overall mechanistic scenario.

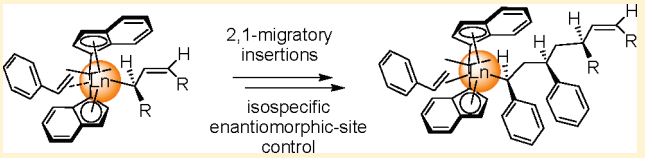

INTRODUCTION

Stereoselective polymerization of styrene has made significant progress over the past two decades, thanks to the development of new families of metal-based catalysts.[1] Syndiotactic polystyrene (sPS) was discovered in 1985 by Ishihara et al. using half-sandwich catalysts, typically binary combinations of mono(cyclopentadienyl)-titanium complexes and MAO.[2] In line with the extensive search for new-generation polymerization catalysts,[3] a range of highly effective single-site catalysts for syndioselective styrene polymerization has appeared in recent years. Of remarkable significance are systems based on post-metallocene titanium complexes supported by amidinate[4,5] or sulfur-bridged bis(phenolate) ligands,[6,7] as well as metallocene and half-sandwich complexes based on group 2 (Ca(II))[8] and even more on group 3 metals, especially Yb(II),[8] Sc(III),[9] and Nd(III).[10,11]

On the other hand, far fewer catalyst systems able to polymerize styrene in a highly isoselective manner have been reported. Isotactic polystyrene (iPS) has long been best produced by heterogeneous catalysis[12] or anionic polymerization,[13] yet still with limited isotacticities. Besides homogeneous catalysts that have been reported to give isotactic *enriched* polystyrene and oligomers,[14] only three examples of true single-site catalysts that form polystyrene *isoselectively* (*mmmm* > 0.9) are known thus far (Scheme 1):[1] (i) the binary system (**A**) based on a *racemic* isopropylidene-bridged bis(benz[e]indenyl) zirconium complex activated by MAO, briefly reported by Arai et al.,[15] (ii) the binary systems (**B**) described by Okuda et al. based on MAO and titanium complexes supported by 1,4-dithiabutane-bridged bis(phenolato) {$OSSO^{2-}$} ligands,[6a−c] and (iii) *racemic* isopropylidene-bridged bis(5-indenyl) yttrium and neodymium allyl complexes (**1**−**4**) of the type {$CMe_2(Ind)_2$}Ln(allyl)$(THF)_n$ (Ind =5-indenyl) developed by Carpentier et al..[16]

The latter compounds, which are analogues of allyl *ansa*-lanthanidocene complexes supported by {$Cp'CMe_2Flu'$}$^{2-}$ (Flu′ = 9-fluorenyl) ligands that allowed the near perfect syndioselective polymerization of styrene,[11] are the first and thus far only reported single-component catalysts for the (almost) perfect isoselective styrene polymerization. In this full account,[16] we describe experimental as well as theoretical studies aimed at exploring the mechanistic details of this polymerization process. The nature of the initiating group, the regioselectivity and stereoselectivity in the initiation and propagation steps, as well as their origin have been investigated by spectroscopic techniques and DFT computations.

Received: February 18, 2011
Revised: March 25, 2011
Published: April 07, 2011

Scheme 1. Single-Site Catalysts for *Isoselective* Styrene Polymerization[6,16]

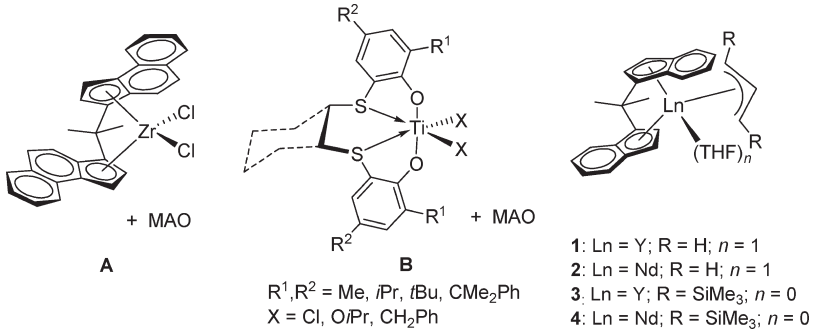

Scheme 2. Isoselective Styrene Polymerization Catalyzed by *Racemic ansa*-Lanthanidocene Allyl Complexes 1−4

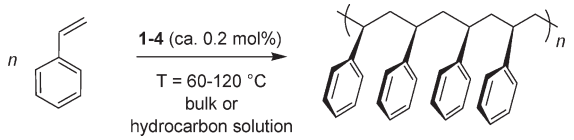

RESULTS AND DISCUSSION

1. General Features of Isospecific Styrene Polymerization Mediated by *Racemic ansa*-Lanthanidocene Allyl Complexes 1−4. Isospecific styrene polymerization was explored with *racemic ansa*-lanthanidocene allyl complexes **1**−**4** (Scheme 1). These four compounds, which differ by the nature of the metal center (yttrium vs. neodymium) and that of the allyl group (unsubstituted vs. 1,3-$(SiMe_3)_2$ disubstituted group), were prepared straightforwardly by a simple one-pot, two-step procedure. The latter procedure involves reaction of the dilithium salt of the isopropylidene-bridged bis(indenyl) ligand with 1 equiv of the lanthanide chloride precursor in ether, and further reaction with 1 equiv of $(C_3H_5)MgCl$ or [1,3-$(SiMe_3)_2$-C_3H_3]K.[16] Their characterization and authentication was achieved by elemental analysis and NMR spectroscopic techniques (see the Experimental Section), as well as by X-ray diffraction studies for compound **3**, confirming, in particular, the *rac*-coordination mode of the isopropylidene-bridged bis(indenyl) ligand.[16] Compounds **3** and **4** derived from the 1,3-$(SiMe_3)_2$ disubstituted allyl ligand contain no coordinated ether (THF, OEt_2) molecule, in contrast to the analogous unsubstituted allyl derivatives **1** and **2** that each bear one such ether molecule; they also proved much more soluble than their nonsubstituted analogues. Polymerizations of styrene with these *racemic ansa*-lanthanidocene allyl complexes were typically carried out in bulk styrene or as concentrated (4.35 M) solutions in cyclohexane or heptane at 60−120 °C, with typically 400−500 equiv of monomer, in the absence of any activator or scavenger (Scheme 2). Representative results are summarized in Table 1 and additional kinetic monitoring experiments are provided in Figures 1−4.

The main features of these polymerizations in terms of catalysis can be summarized as follows: (i) all complexes **1**−**4** were found to be active in the temperature range 60 to 120 °C, giving essentially pure isotactic polystyrene (*mmmmmm* > 0.99, *vide infra*) as *crude* material (i.e., no fractionation was required); (ii) catalytic productivities (calculated on the basis of the amount of allyl compound introduced) were in the range 40−1,600 $kg(iPS)\cdot(mol(Ln)\cdot h)^{-1}$, with **3** ≥ **4** > **1** > **2**, and these productivities expectedly increased with temperature; (iii) polymerizations conducted with **1** and **2** proceeded without induction period, in contrast to those promoted with **3** and **4** that evidenced time periods of a few minutes before polymerization took place (Figures 1 and 2), irrespective of the conditions (neat styrene or 4.35 M solutions in hydrocarbons; 60−100 °C); (iv) all polymers featured symmetric, monomodal GPC traces, indicative of a single-site behavior of the catalyst; yet, complexes **3** and **4** led to somewhat broader polydispersities (typically, M_w/M_n = 2.2−2.6) as compared to those observed with **1** and **2** (M_w/M_n = 1.5−2.0); (v) higher polymerization temperatures induced a decrease of the M_n values, usually accompanied by a slight broadening of the polydispersities; (vi) the molecular weights M_n showed monotonous dependence on monomer conversion, with an almost linear relationship (at least in the first stages of the polymerization) for the neodymium catalyst **2**, but an obvious saturation limit for yttrium compounds **1** and **3** (Figures 3 and 4); (vii) somewhat lower catalytic productivities were achieved when polymerizations were carried out in cyclohexane or heptane solutions (instead of bulk styrene), but the recovered polymers showed essentially identical isotacticity indices and very similar molecular weights and molecular weight distributions.

Overall, these observations indicate that compounds **1**−**4** exert a significant degree of control over styrene polymerizations in terms of isotacticity and molecular weights. However, several limitations and peculiar behaviors must be noted: First, the broadening of molecular weight distributions and reduction of molecular weights at higher temperatures, as well as saturation of molecular weights vs. conversions, especially noticeable in the case of yttrium compounds **1** and **3**, reflect that transfer reactions (e.g., to the monomer) and termination processes (β-H elimination) take place to a significant extent under those conditions. Moreover, the induction periods and relatively broad molecular weight distributions observed when using **3** and **4** suggest a more difficult initiation with these complexes. This is probably due to the presence of a relatively more bulky 1,3-$(SiMe_3)_2$ disubstituted allyl group in the latter compounds, as compared to the simple allyl group present in compounds **1** and **2**, that hinders the monomer approach/insertion; electronic factors may also account for the lower reactivity (stabilization by negative hyperconjugation with the $SiMe_3$ groups). This hypothesis was confirmed by ^{1}H NMR monitoring of the addition of 3 equiv of styrene to a cyclohexane-d_{12} solution of **3** at 25 °C, which revealed that propagation proceeds faster than initiation [i.e., formation of iPS rather than single styrene insertion product was

dx.doi.org/10.1021/ma2003757 |*Macromolecules* 2011, 44, 3312–3322

Table 1. Isoselective Styrene Polymerization Catalyzed by *Racemic ansa*-Lanthanidocene Allyl Complexes 1−4[a]

entry	compd	$[St]_0/[Ln]_0$	temp [°C]	time [min]	convn [%]	productivity[b]	M_n[c]	M_w/M_n[c]
1	**1**	500	60	2	8	123	42	1.46
2	**1**	500	60	5	24	135	59	1.59
3	**1**	500	60	10	39	121	81	1.69
4	**1**	500	60	15	44	93	94	1.63
5	**1**	500	60	20	65	95	89	1.83
6[d]	**1**	500	60	60	58	27	59	1.58
7	**1**	500	80	15	87	181	58	1.85
8	**1**	500	100	5	92	527	26	1.72
9	**1**	400	120	5	88	463	28	2.03
10	**2**	500	60	5	5	355	32	1.15
11	**2**	500	60	10	16	55	67	1.29
12	**2**	500	60	15	29	60	83	1.39
13	**2**	500	60	20	30	52	109	1.41
14	**2**	500	60	30	39	49	125	1.63
15	**2**	500	60	50	59	37	158	1.79
16[d]	**2**	600	60	60	26	16	87	1.52
17	**2**	600	100	5	43	307	52	1.60
18	**3**	450	60	8	11	39	59	2.24
19	**3**	460	80	4	95	685	46	2.41
20[d]	**3**	470	80	10	95	283	61	1.92
21	**3**	420	100	2	98	1 279	22	2.53
22	**3**	480	120	2	100	1 637	12	3.45
23	**4**	500	60	8	100	392	71	2.63
24	**4**	520	80	6	100	600	56	2.51
25[d]	**4**	510	80	15	65	140	120	1.81
26	**4**	480	100	5	100	1 094	36	2.27

[a] General conditions unless otherwise stated: 20−40 μmol Ln, styrene volume 2.0 mL, $[styrene]_0$ = 8.70 M (neat). [b] Productivity in kg(PS)·(mol(Ln)·h)$^{-1}$. [c] M_n [10^3 g·mol^{-1}] and M_w/M_n determined by GPC in THF vs PS standards. [d] Reaction run at $[styrene]_0$ = 4.35 mol·L^{-1} in cyclohexane or heptane (1:1 *v*/*v* styrene/hydrocarbon solution).

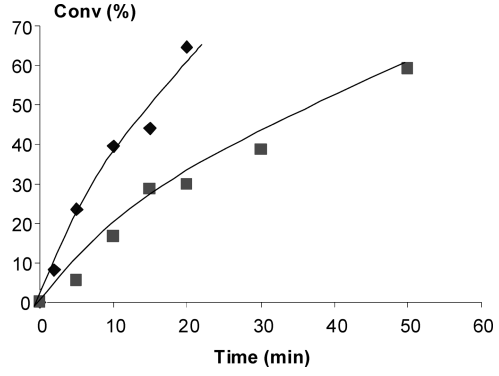

Figure 1. Representative kinetic profiles of styrene polymerizations catalyzed by compounds **1** (◆) and **2** (■) (60 °C, $[styrene]_0/[Ln]_0$ = 500, neat styrene; see Table 1).

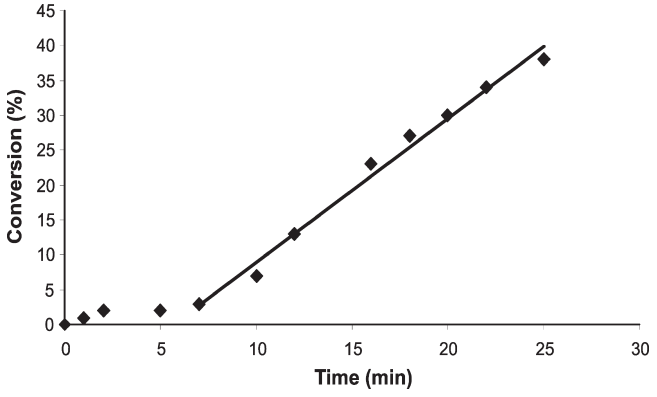

Figure 2. Representative kinetic profile of a styrene polymerization catalyzed by compound **3** (80 °C, $[styrene]_0/[Y]_0$ = 500, 1:1 (v/*v*) heptane:styrene solution; see Table 1).

observed] but that only a minor part of the catalyst is active under these conditions [i.e., significant amounts of iPS were produced although allyl compound **3** was still the only detectable yttrium species]. It is also noteworthy that the experimental M_n values obtained for polymerizations promoted by complex **3** were higher than the M_n values calculated from the styrene-to-catalyst ratio and conversion, thus corroborating the poor initiation efficiency of this complex.

2. Microstructural Analyses of Isotactic Polystyrenes Produced from Allyl *ansa*-Lanthanidocene Complexes 1−4. In order to get more insight into the mechanism operative in these polymerizations, the microstructure of the isotactic polystyrenes produced was investigated in details by spectroscopic techniques. Our aims were to determine the nature of the initiating group, the regioselectivity (secondary vs primary) of monomer enchainment in the initiation and propagation steps, and the

dx.doi.org/10.1021/ma2003757 |*Macromolecules* 2011, 44, 3312–3322

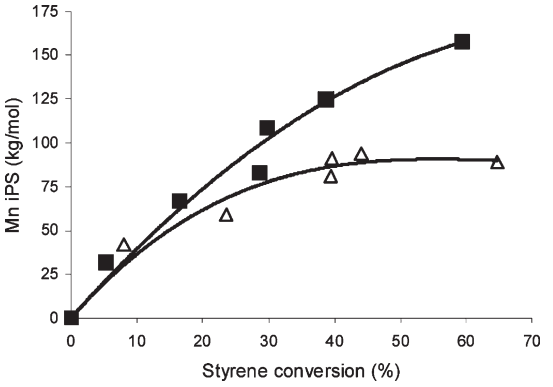

Figure 3. Dependence of M_n values of iPS vs. styrene conversion for compounds **1** (△) and **2** (■) (60 °C, $[\text{styrene}]_0/[\text{Ln}]_0$ = 500; neat styrene; see Table 1).

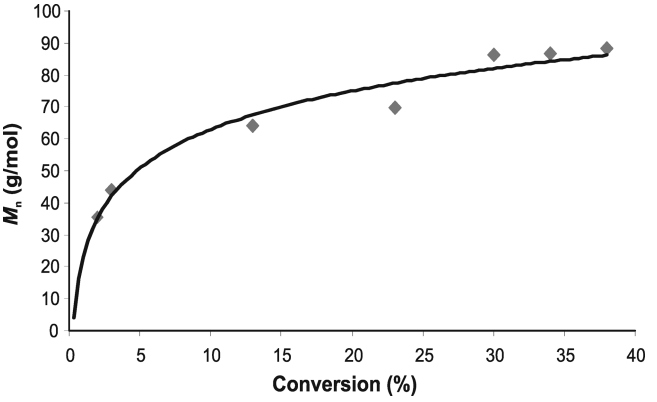

Figure 4. Dependence of M_n of iPS vs. styrene conversion catalyzed by compound **3** (80 °C, $[\text{styrene}]_0/[\text{Y}]_0$ = 500, 1:1 (v/v) heptane/styrene solution; see Table 1).

stereocontrol mechanism (enantiomorphic site vs. chain-end) operative in this process.

2.1. Nature of Polystyrene End-Groups and Regioselectivity of Monomer Enchainment. The ^{1}H NMR spectrum of a low molecular weight polystyrene ($M_n = 6 \times 10^3$ g·mol^{-1}, as determined by GPC) produced with complex **2** ($[\text{styrene}]_0/[\text{Nd}]_0$ = 20, neat styrene, 60 °C, 30 min), and carefully reprecipated to eliminate as much as possible residual impurities, showed the resonances characteristic for allyl-terminated chains (δ 5.63 (1H) and 4.82 ppm (2H)), Figure 5). The chemical shifts observed for this terminal allyl group are actually very similar to those observed for terminal allyl groups in *syndiotactic* polystyrenes (δ 5.59 (1H) and 4.81 ppm (2H)) produced with single-component *ansa*-neodymocene allyl complexes of the type {Cp′CMe$_2$Flu′}Nd(allyl)(THF).[11c] The molecular weight of the polymer determined by NMR from this allyl end-group ($M_{n,NMR}$ = 7.5 × 10^3 g·mol^{-1}) was in good agreement with the one determined by GPC ($M_{n,GPC} = 6 \times 10^3$ g·mol^{-1}).

The presence of allyl end-groups was further confirmed by MALDI−ToF mass spectroscopy analyses: in the mass spectra, a single distribution was observed (Figure 6) and the molecular weight of each peak was consistent with the calculated molecular weights for the on-matrix compounds (H)(C$_8$H$_8$)$_n$-(C$_3$H$_5$)Ag, where *n* represents the degree of polymerization (Table 2).

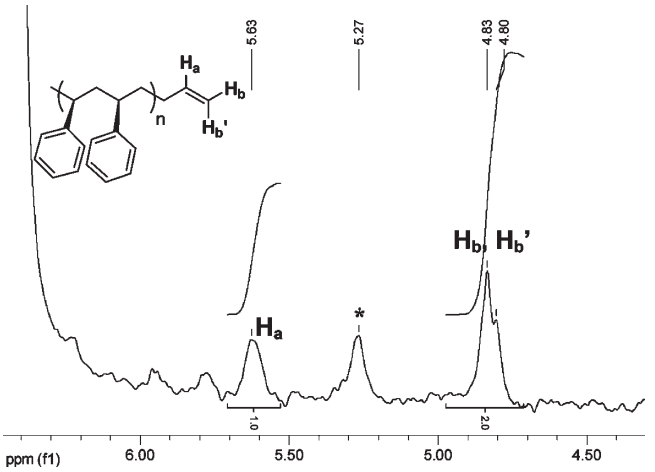

Figure 5. ^{1}H NMR spectrum (500 MHz, 25 °C, $CDCl_3$) of a low molecular weight H-iPS-allyl prepared with complex **2** ($[\text{styrene}]_0/[\text{Nd}]_0$ = 20, neat styrene, 60 °C, 30 min) (∗ is an unidentified resonance).

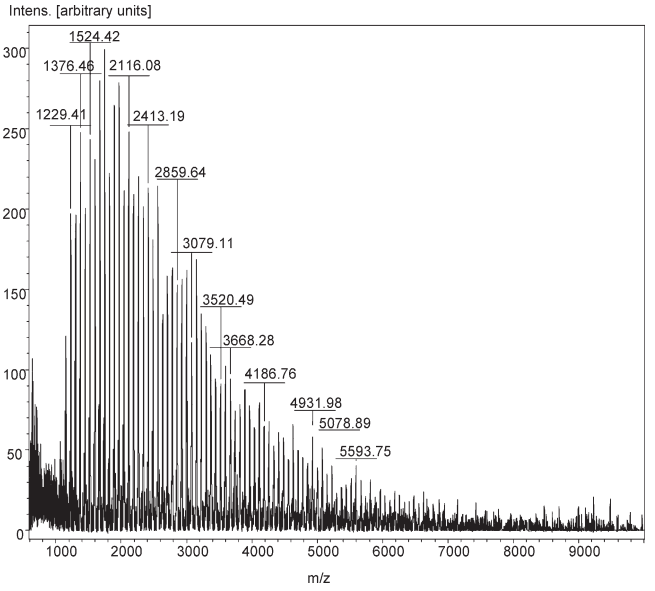

Figure 6. MALDI−ToF mass spectrum of a low molecular weight H-iPS-allyl prepared with complex **2** ($[\text{styrene}]_0/[\text{Nd}]_0$ = 20, neat styrene, 60 °C, 30 min) (polymer doped with AgOTf, dithranol matrix (note that the molecular weights observed were somewhat lower than the ones obtained by GPC, which likely stems from a better ionization of shorter chains and/or better cocrystallization with the matrix compound).

It can be concluded therefore that styrene polymerization mediated by these *racemic* isopropylidene-bridged bis(indenyl) lanthanide allyl complexes is initiated by styrene insertion into the allylic metal−carbon bond. However, the above ^{1}H NMR and MS analyses did not allow to discriminate CH$_2$═CH−CH$_2$−CH(Ph)−CH$_2$− and CH$_2$═CH−CH$_2$−CH$_2$−CH(Ph)− end groups and thus to assess the regioselectivity (primary or secondary insertion mode) of the first insertion of styrene.

In order to clarify the regiochemistry of the styrene insertion in both the initiation and propagation steps, low-molecular weights

dx.doi.org/10.1021/ma2003757 |*Macromolecules* 2011, 44, 3312–3322

Table 2. MALDI−ToF−MS Data of a Low Molecular Weight H-iPS-Allyl Prepared with Complex 2 ($[styrene]_0/[Nd]_0 = 20$, Neat Styrene, 60 °C, 30 min)

polymerization degree [n]	calculated mass [g mol^{-1}]	observed mass [g mol^{-1}]
40	4313	4315
41	4417	4418
42	4521	4524
43	4625	4627
44	4728	4732
45	4834	4836

Table 3. Preparation of H(D)-iPS-*n*Bu Samples *via* Isoselective Coordinative Chain Transfer Polymerization of Styrene Mediated by the Combination 3/Mg(nBu)$_2$[a]

entry	[Y]/[Mg]/[St]	styr convn [%]	iPS yield [g]	M_n[b]	M_w/M_n[b]	iPS/Y[c]
1[d]	1:10:2000	97	7.0	5.6	1.5	36
2[e]	1:10:2000	94	6.8	4.8	1.6	41

[a] Polymerization conditions: **3** (35 μmol), heptane (5 mL), 80 °C, 60 min. [b] M_n [10^3 g mol^{-1}] and M_w/M_n determined by GPC in THF vs PS standards. [c] Number of iPS chains formed per Y center. [d] Polymerization quenched with a 1:1 (v/v) solution of CH_3CO_2H and CH_3OH. [e] Polymerization quenched with a 1:1 (v/v) solution of CF_3CO_2D and CH_3OD.

iPS samples were prepared via "coordinative chain-transfer polymerization" (CCTP) using compound **3** as isoselective catalyst and di(*n*-butyl)magnesium as chain transfer agent (CTA). It is well-known in the literature that, under appropriate conditions, the use of an alkyl-metal MR_n as CTA (such as $ZnEt_2$, Mg(nBu)$_2$, $AlEt_3$, ...) in polymerization does not alter the nature of the catalytically active species but allows for a fast and reversible (when effective) intermolecular chain transfer of growing polymer chains, eventually leading to the formation of M(polymeryl)$_n$ species, where the polymeryl chains are selectively capped with R end-groups.[17,18] We previously used such an approach to prepare Mg(sPS-nBu)$_2$ species and analyze accurately the monomer enchainment mode in H(D)-sPS-*n*Bu, obtained after quenching these reactive *syndiotactic* polystyrenyl chains with either protonated or deuterated agents.[11c]

The polymerization conditions and characteristics of the H(D)-iPS-*n*Bu samples prepared following this CCTP protocol, using the binary system 3/Mg(nBu)$_2$ (1:10), are gathered in Table 3. The $^{13}C\{^1H\}$ NMR spectrum of the low molecular weight H-iPS-*n*Bu obtained after regular protonolysis (Table 3, entry 1) showed a single series of intense resonances for the highly isotactic polymer backbone; no signals for head-to-head or tail-to-tail sequences were detected, confirming that the polymerization is highly regioselective in both the initiation and propagation steps. Besides those signals for the polymer backbone, a series of low intensity signals was observed (see Figure S3, Supporting Information and Figure 7). The resonances at δ 14.2, 22.6, 27.1, 31.8, 35.6, and 45.8 ppm were unambiguously assigned to a 1-phenylhexyl (i.e., 2,1-St-*n*Bu) end-group, on the basis of the literature;[11c,19] in particular, the signals at δ 35.6 and at 45.8 ppm were assigned, respectively, to the methylene and methine of the first monomer units, in agreement with data

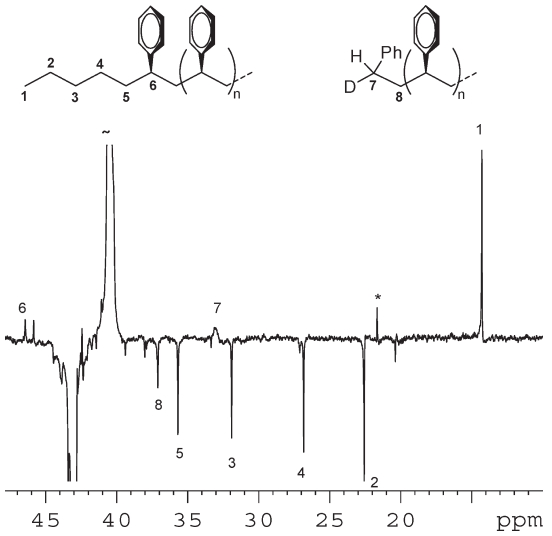

Figure 7. Detail of the aliphatic region of the Dept-135 $^{13}C\{^1H\}$ NMR spectrum (125 MHz, $C_2D_2Cl_4$, 25 °C) of a deuterium end-labeled D-iPS-*n*Bu sample (Table 3, entry 2) (the * marker refers to residual toluene resonance), with details of the expected termini following secondary insertion and propagation and quenching with CF_3COOD/CH_3OD.

reported for styrene units adjacent to ethylene-ethylene sequences in ethylene/styrene copolymers.[19] Overall, these data confirm the effectiveness of the CCTP process operating between **3** and Mg(nBu)$_2$ and, more importantly, establish that the first insertion of styrene is highly regioregular and is secondary (Scheme 3).

Information concerning the regiochemistry in the propagation step was derived from analysis of the opposite chain end-group in the H(D)-iPS-*n*Bu samples. Indeed, hydrolysis of Mg(iPS-nBu)$_2$ species resulting from primary and secondary growing PS chains leads to different chain end-groups (Scheme 3). In the $^{13}C\{^1H\}$ NMR spectrum of the H-iPS-*n*Bu sample (Table 3, entry 1), the two signals in the aliphatic region at δ 33.0 and 37.1 ppm were assigned to the methylene of the chain end-group $PhCH_2CH_2$− polymer, formed after hydrolysis of *secondary* growing iPS chains.[11c] To confirm this assignment and rule out the presence of other chain end-groups, a deuterium labeling experiment was performed by quenching the polymerization with a 1:1 mixture of CF_3COOD and CH_3OD (Table 3, entry 2). The ^2H NMR spectrum of the resulting D-iPS-*n*Bu showed a single resonance at δ 2.2 ppm, attributable to $PhCHDCH_2$−polymer, and clearly indicative of the presence of only one termination pathway (see the Supporting Information). In addition, the $^{13}C\{^1H\}$ and Dept-135 ^{13}C NMR spectra of this D-iPS-*n*Bu were identical to those of the protonated analogue, except for the signal at δ 33.0 ppm originally assigned to a $PhCH_2CH_2$−polymer chain end group (*vide supra*): the narrow downward signal in H-iPS-*n*Bu turned into a broad upward signal in D-iPS-*n*Bu, diagnostic of the terminal $PhCHDCH_2$− unit (Figure 7).

These experimental data allowed us to conclude that the isospecific polymerization of styrene promoted by **3**/Mg(nBu)$_2$, and more generally by single component *ansa*-lanthanidocene allyl complexes **1**−**4**, is highly regioselective and proceeds in a 2,1-insertion mode, both in the initiation and propagation steps.

2.2. Microstructure of the Polystyrene Backbone and Stereocontrol Mechanism. The microstructure of the polystyrenes

Scheme 3. Possible Insertion, Propagation, and Chain Transfer Pathways for Secondary or Primary Growing Chains

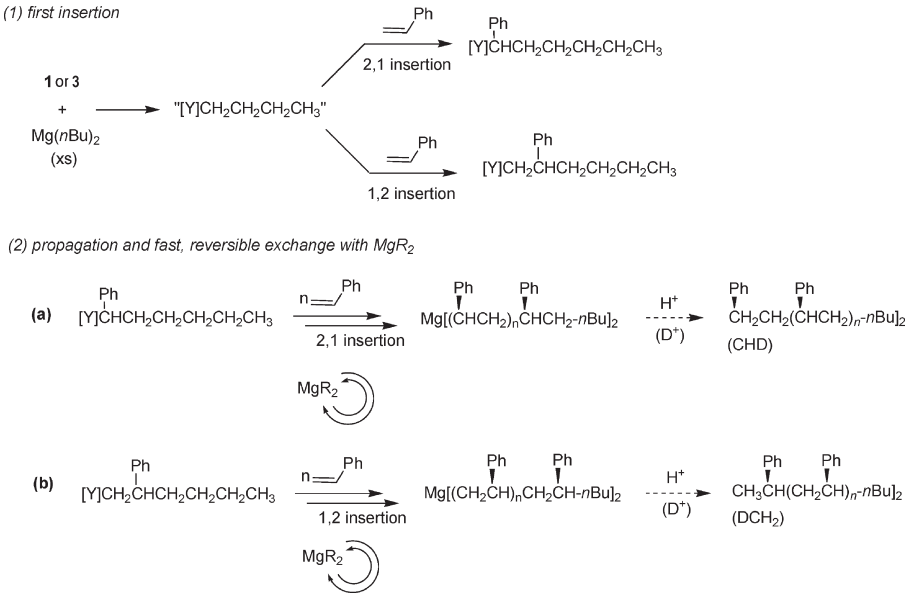

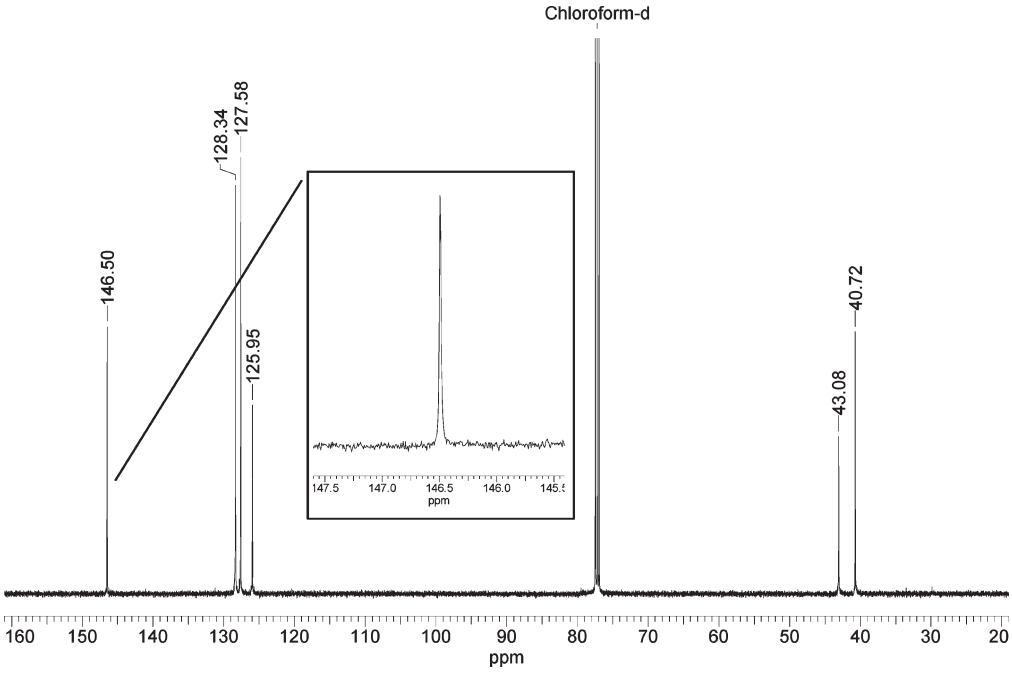

Figure 8. $^{13}C\{^{1}H\}$ NMR spectrum (125 MHz, 40 °C, $CDCl_3$) of a crude iPS sample prepared at 100 °C with complex **2** (Table 1, entry 17).

prepared with complexes **1**−**4** was determined by $^{13}C\{^{1}H\}$ NMR spectroscopy. A typical spectrum of an *unfractionated* polymer produced at 120 °C is shown in Figure 8. This spectrum features a single sharp resonance at δ = 146.50 ppm assigned to the aromatic *ipso* carbon in a *mmmmmm* heptad.[20] This indicates the highly isotactic microstructure of those materials, as corroborated from the melting temperatures (T_m = 219−222 °C)[6] determined by DSC analysis (see the Supporting Information).

Besides the strong resonance for the *mmmmmm* heptad (**A**), polystyrenes produced with compounds **1**−**4** at temperatures above 120 °C featured four additional resonances (**B**−**E**), of roughly equal intensity (1.6, 1.0, 1.0, 1.1, respectively), in the aromatic *ipso* carbon region of the ^{13}C NMR spectrum (Figure 9). These reflect stereoerrors that occurred during the polymerization process at more elevated temperatures. At this stage, it is worth mentioning that the configurationally flexible catalyst $[Ti(mdtbp)(CH_3)_2]/B(C_6F_5)_3$ [mdtbp = $(OC_6H_2$-tBu$_2$-4,6$)_2(SCH_2S)$] with a methylene-bridged $\{OSCH_2SO\}^{2-}$ backbone produced iPS whose $^{13}C\{^{1}H\}$ NMR spectra are *rigorously* identical to that shown in Figure 9. These one-carbon bridged catalysts $[Ti(mdtbp)(CH_3)_2]/B(C_6F_5)_3$ generate at 60 °C iPS with the *same* ^{13}C NMR signal pattern (i.e., number,

dx.doi.org/10.1021/ma2003757 |*Macromolecules* 2011, 44, 3312–3322

chemical shifts and intensities) of stereoerrors than those produced with compounds **1**-**4**.[21,22] This striking similarity between the ^{13}C NMR fingerprints of these iPS prepared with entirely different catalyst types rules out the possibility of an impurity accounting for any of these additional resonances; rather, it points at an inherently identical microstructure and hence related enantiomorphic site stereocontrol mechanism.

In fact, three of the additional resonances observed in iPS produced at higher temperatures were confidently assigned at the heptad level on the basis of literature data: signals at δ = 146.32 (**B**), 146.23 (**D**), and 145.78 (**E**) ppm correspond to *mmmmmr*, *mmmmrr*, and *mmmrrm* heptads, respectively. The observed chemicals shifts match indeed well those reported by Harwood et al. and further confirmed by others for isotactic-enriched PS (δ = 146.32, 146.20, and 145.77 ppm, respectively).[20] Resonances **B**, **D**, and **E** correspond in a site-controlled mechanism to the three most intense of the four erroneous heptads formed after a single stereochemically "wrong" insertion. The fourth resonance for the *mmrrmm* heptad, anticipated in such stereocontrol mechanism, was tentatively assigned to signal **C** at δ 146.26 ppm.[23] In previous works,[20] this *mmrrmm* heptad was assigned to a much higher field resonance (δ = 144.97 ppm). Yet, this initial assignment seems erroneous in light of our NMR spectra of iPS produced from both Y and Ti catalysts, in which signals at δ = ca. 145.0 ppm were barely observable.

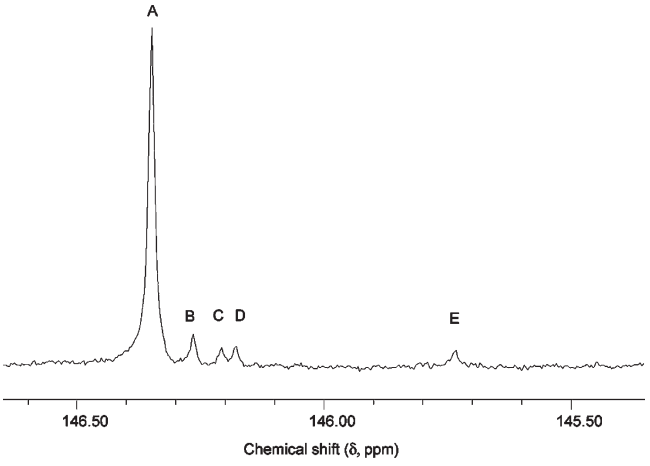

Figure 9. Detail of the phenyl *ipso* carbon region of the $^{13}C\{^1H\}$ NMR spectrum (125 MHz, 60 °C, $CDCl_3$) of an iPS sample prepared at 125 °C with complex **2**.

3. DFT Computations. In order to confirm the regioselectivity and stereoselectivity of the first two insertions, and the overall mechanistic scenario envisioned on the basis of the above experimental data, DFT computations were performed. The methodology of these computations is identical to the one we recently used to assess in details the mechanism of the syndioselective polymerization of styrene with *ansa*-lanthanidocene allyl complexes supported by $\{Cp'CMe_2Flu'\}^{2-}$ ligands.[11c] The bis(silyl)-substituted allyl yttrium complex **3** was selected for these computations as this compound does not carry a THF molecule (in contrast to **1** and **2**) and therefore does not require to hypothesize a preliminary decoordination to liberate a vacant site for the incoming monomer. Moreover, it will allow to assess the aforementioned suggestion that the first monomer insertion in these highly congested allyl compounds (**3**, **4**) is more demanding than subsequent insertions. Thus, two consecutive styrene insertions on one enantiomer of complex **3** were computed (see the Experimental Section for details) and the different free energy profiles are presented in Scheme 4. It must be first noted that the DFT-optimized structure of compound **3** matches well that determined by X-ray diffraction studies[16] (Cp−Y−Cp bite angle =113.0 vs. 113.3°; Y−C(allyl) = 2.57−2.61 vs. 2.57−2.58 Å; see the Supporting Information for a complete list of atomic coordinates).

For the first monomer insertion, the four possible scenarios were considered, namely 1,2- vs. 2,1- with *Re vs. Si* insertion of styrene (Scheme 5). There is a slight (within the precision of the method) preference for the 2,1-*Si* insertion, although all four insertions were computed to be quite comparable in energy. The geometry of the corresponding transition states is also quite similar and reveals, as anticipated, a marked elongation of the

Scheme 4. Free Enthalpy Profiles of the First and Second Insertions of Styrene in *rac*-$\{CMe_2(Ind)_2\}Y(1,3\text{-}(SiMe_3)_2C_3H_3)$ (3)

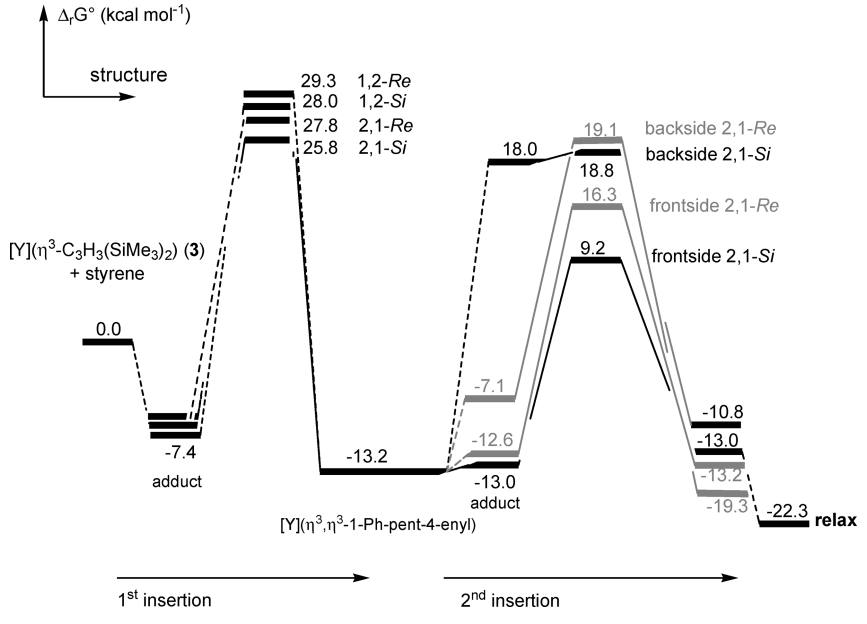

dx.doi.org/10.1021/ma2003757 |*Macromolecules* 2011, 44, 3312–3322

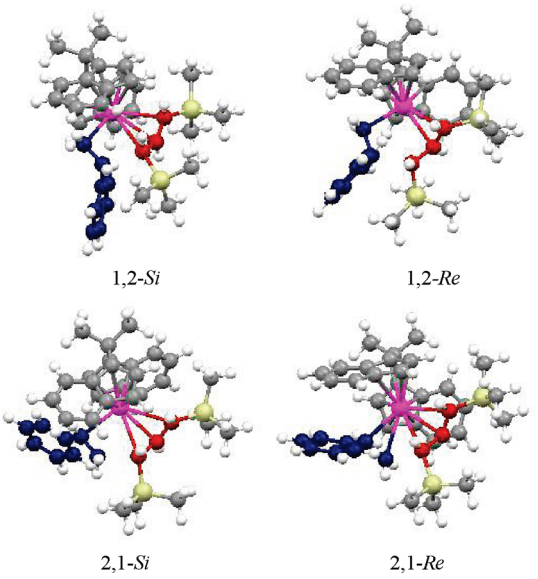

Figure 10. Optimized geometries of the four transition states for the first insertion of styrene in *rac*-{$CMe_2(Ind)_2$}Y(1,3-$(SiMe_3)_2C_3H_3$) (**3**).

Scheme 5. Orientation Modes and Nomenclature Used for Styrene Insertion with Respect to the Ancillary Ligand

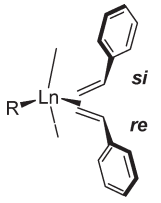

Y−C(allyl) bond distances (e.g., 2.69−2.83 Å in TS-2,1-*Re* and 2.69−2.78 Å in TS-2,1-*Si*) but a slight narrowing of *ca.* 3° of the Cp-Y-Cp bite angle (Figure 10). The close similarity of the geometries within these four scenarios and with the metal−ligand core in the initial complex (**3**) reflects good accessibility of the coordination site to the incoming monomer. This reduces in turn the steric interaction between the incoming styrene and the ancillary ligand, which accounts for the similar activation energies computed for the four scenarios at this stage of the process. In all cases, the energy barriers for this first insertion were found to be accessible (*ca.* 33−37 kcal·mol^{-1} with respect to the styrene adduct). The reaction was also computed to be exergonic by 13 kcal·mol^{-1} (vs. **3** + styrene).

For the second insertion, we considered frontside "migratory" vs. backside "stationary" styrene insertions from the 2,1-*Si* first insertion product. To simplify the study, in accordance with the results found on the first insertion (*vide supra*) and those obtained in the DFT modeling of the syndioselective polymerization with related Cp-Flu systems,[11c] only the 2,1-insertions were considered. Results of computations on these four possibilities revealed a clear kinetic preference for a frontside 2,1-*Si* second insertion, resulting in an isotactic enchainment of the monomer units; the other three possibilities were at least 7 kcal·mol^{-1} more demanding (Scheme 4). A close examination of the transition state geometries did not reveal obvious differences

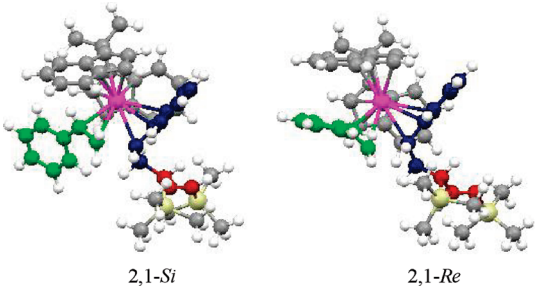

Figure 11. Optimized geometries of the two transition states for the second frontside "migratory" 2,1-insertion of styrene in *rac*-{$CMe_2(Ind)_2$}Y(1,3-$(SiMe_3)_2C_3H_3$) (**3**).

between the two most favored ones (TS-2,1-*Si* and TS-2,1-*Re*) for the Y···(styrene) and C(styrene)···C(growing chain) contacts (Figure 11). It should be noted that, unlike the syndioselective polymerization with the Cp-Flu systems,[11c] the two migratory insertions were found to be preferred with respect to the stationary insertion; this can be likely attributed to the homotopicity of both coordination sites connected with the C_2 symmetry of the ligand. The energy barrier of *ca.* 22 kcal·mol^{-1} was found to be much more accessible than that for the first insertion. This is in agreement with the more difficult initiation for those compounds bearing a bulky allyl group [i.e., **3** and **4**, as compared to **1** and **2**, which are based on the unsubstituted allyl moiety], in line with experimental kinetic observations and broader molecular weight distributions. It is also noteworthy that the latter energy barrier of *ca.* 22 kcal·mol^{-1} is comparable to those reported for the syndioselective polymerization with Cp-Flu allyl catalysts.[11c] The second insertion step in a frontside 2,1-*Si* mode leads to a product that features the last inserted styrene unit in a alkyl-(eta-1) type coordination mode and a somewhat constrained growing chain (Figure 12). However, further relaxing the chain offered a product with the anticipated η-3 coordinated styrene moiety and resulted in an extra stabilization of 9.3 kcal·mol^{-1}; the latter value provides a first estimate of the polymerization energy.

4. Concluding Remarks. *Racemic ansa*-bis(indenyl) allyl yttrium and neodymium complexes **1**−**4** are unique single-site and single-component catalysts for the preparation of highly isotactic polystyrene with a broad range of molecular weights and distributions, under synthetically attractive conditions (solvent-free or high concentrations of styrene, 60−120 °C). A detailed analysis of the end-groups in the formed iPS chains, combined with DFT studies, allowed us to conclude on a pure coordinative−insertive polymerization mechanism of styrene into the metal−carbon(allyl). More, styrene insertion is highly regioselective and proceeds in secondary mode, both in the initiation and propagation steps. In these regards, those isospecific systems behave similarly to *ansa*-{CMe_2(Cp-Flu)}Nd(allyl)(THF) that has proved particularly efficient for the syndioselective polymerization of styrene. ^{13}C NMR microstructural analyses of the iPS are consistent with an enantiomorphic site control of the polymerization, in line with the *rac*-coordination of the $\{CMe_2(Ind)_2\}^{2-}$ ligand in these compounds. This stereocontrol mechanism is also operative with some Ti-{OSSO}-type catalysts that generate iPS featuring rigorously the same ^{13}C NMR fingerprint of stereorrors.[21] On that basis, a partial revision of the assignment of ^{13}C NMR resonances has been proposed.

dx.doi.org/10.1021/ma2003757 |*Macromolecules* 2011, 44, 3312–3322

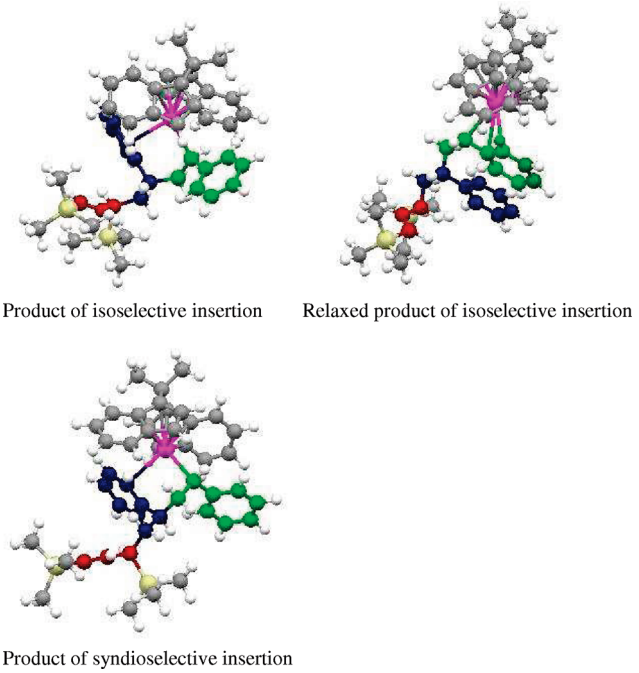

Figure 12. Optimized geometries of the products for the first and second frontside "migratory" 2,1-insertion of styrene in *rac*-{CMe_2-$(Ind)_2$}Y(1,3-$(SiMe_3)_2C_3H_3$) (**3**).

EXPERIMENTAL SECTION

General Data. All manipulations were performed under a purified argon atmosphere using standard Schlenk techniques or in a glovebox. Solvents were distilled from Na/benzophenone (THF, Et_2O) and Na/K alloy (toluene, pentane, heptane, cyclohexane) under argon, degassed thoroughly and stored under argon prior to use. Deuterated solvents (benzene-d_6, toluene-d_8, THF-d_8, $CDCl_3$, $C_2D_2Cl_4$; all >99.5% D, Eurisotop) were vacuum-transferred from Na/K alloy or CaH_2 into storage tubes. Styrene (Acros) was dried over CaH_2 and distilled under reduced pressure prior to polymerization experiments. The pro-ligand {IndCMe$_2$Ind}H_2 was generously provided by Total Petrochemicals Research. 1,3-$(SiMe_3)_2C_3H_3K$ was prepared according to literature.[24] All other reagents were purchased and used as received.

Instruments and Measurements. ^{1}H, ^{13}C{^{1}H}, and ^{1}H−^{13}C HMBC and HMQC NMR spectra of complexes were recorded on Bruker AC-300 and AM-500 spectrometers in 5 mm Teflon-valved NMR tubes at room temperature unless otherwise indicated. ^{1}H and ^{13}C chemical shifts are reported vs $SiMe_4$ and were determined by reference to the residual solvent peaks. Coupling constants are given in Hertz. Elemental analyses (C, H, N) were performed using a Flash EA1112 CHNS Thermo Electron apparatus and are the average of two independent determinations.

^{13}C{^{1}H} NMR analyses of polymers were performed in $CDCl_3$ (or $C_2D_2Cl_4$) at 25 °C (or 40 °C) in 5 mm tubes on AM-500 and AC-300 Bruker spectrometers operating at 125 and 75 MHz, respectively; spectra were recorded in the inverted-gate decoupling-acquisition mode with the following parameters: delay 30 s, acquisition time 1.18 s, number of scans ≥2000.

GPC analyses of polymers were performed in THF (1.0 mL·min^{-1}) at 30 °C on a Polymer Laboratories PL50 apparatus equipped with PLgel 5 μm MIXED-C 300 × 7.5 mm columns, and combined RI and Dual angle LS (PL-LS 45/90°) detectors. The number-average molecular masses (M_n) and polydispersity index (M_w/M_n) of the polymers were calculated with reference to a universal calibration vs polystyrene standards.

MALDI−ToF−MS analyses were performed on a AutoFlex LT spectrometer (Bruker Daltonics) which was operated in the linear (19 kV) mode. The spectra were recorded in the positive-ion mode. The samples were prepared by taking 2 μL of a THF solution of the polymer (10 mg PS·mL^{-1}) and adding this to 16 μL of 1,8-dihydroxy-9(10*H*)-anthracenone (dithranol, 10 mg·mL^{-1} in THF) to which had been added 2 μL of CF_3SO_3Ag (2 mg·mL^{-1} in THF). A 1 μL portion of this mixture was applied to the target and 50−100 single shot spectra were accumulated. Given masses represent the average masses of the Ag^+ adducts. The spectrometer was calibrated with an external mixture of angiotensin I, ACTH 18−39 and bovine insulin or PEG 1500.

Differential scanning calorimetry (DSC) analyses were performed on a Setaram DSC 131 apparatus at a rate of 10 °C·min^{-1}, under continuous flow of helium (25 mL·min^{-1}), using aluminum capsules.

***Rac*-{$CMe_2(Ind)_2$}$Y(C_3H_5)(THF)$ (1).** To a solution of {CMe_2-$(Ind)_2$}H_2 (0.437 g, 1.6 mmol) in diethyl ether (20 mL) at −10 °C was added under vigorous stirring 2 equiv of *n*BuLi (2.0 mL of a 1.6 M solution in hexane, 3.2 mmol). The mixture was gently warmed to room temperature. The solution turned green and after 3 h a yellow-green crystalline powder precipitated. To this suspension of the dilithium salt in diethyl ether was added a suspension of $YCl_3(THF)_{3.5}$ (0.716 g, 1.6 mmol) in diethyl ether (20 mL). Upon vigorous stirring and warming to room temperature, the mixture turned bright yellow. Volatiles were removed *in vacuo* to give a yellow powder. To this powder in toluene (20 mL) was added a solution of allylmagnesium chloride (0.80 mL of a 2.0 M solution in THF, 1.6 mmol). The mixture was stirred for 8 h at room temperature. The resulting yellow solution was filtered and volatiles were removed *in vacuo*. The residue was washed with pentane (2 × 15 mL) and dried *in vacuo* to give **1** as a yellow powder (0.64 g, 76%). Anal. Calcd (%) for $C_{28}H_{31}OY$ (472.46): C 71.18, H 6.61; found C 71.5, H 6.75. The ^{1}H NMR spectra of complex **1** in C_6D_6, toluene-d_8 or THF-d_8 in the temperature range −20 to +70 °C were quite complicated, all featuring very broadened resonances, probably as a result of fluxional phenomena; apart from confirming the presence of one coordinated THF molecule, these data were uninformative.

***Rac*-{$CMe_2(Ind)_2$}$Nd(C_3H_5)(THF)$ (2).** Complex **2** was prepared using a similar procedure as that described above for **1**, starting from {$CMe_2(Ind)_2$}H_2 ligand (0.436 g, 1.6 mmol), $NdCl_3(THF)_2$ (0.632 g, 1.6 mmol) and allylmagnesium chloride (1.0 mL of a 2.0 M solution in THF, 2.0 mmol), and isolated as a pale green powder (0.59 g, 70%). Because of the strong paramagnetism of Nd and possible fluxional phenomena, ^{1}H NMR featured only very broad, uninformative resonances. Anal. Calcd (%) for $C_{28}H_{31}ONd$ (527.80): C, 63.72; H, 5.92. Found: C, 63.2; H, 6.15.

***Rac*-{$CMe_2(Ind)_2$}$Y(1,3\text{-}(SiMe_3)_2C_3H_3)$ (3).** To a solution of {$CMe_2(Ind)_2$}H_2 (0.546 g, 2.0 mmol) in Et_2O (50 mL) at −20 °C was added under vigorous stirring 2 equiv of *n*BuLi (2.5 mL of a 1.6 M solution in hexane, 4.0 mmol). The reaction mixture was gently warmed to room temperature. The solution turned green and after 3 h a yellow-green crystalline powder precipitated. To this suspension of the dilithium salt in ether cooled to −20 °C was added a suspension of $YCl_3(THF)_{3.5}$ (0.895 g, 2.0 mmol) in Et_2O (50 mL). Upon vigorous stirring and warming to ambient temperature, the reaction mixture turned bright yellow. The solution was decanted from the precipitate, filtered, and evaporated *in vacuo* to give a yellow powder. To a suspension of this powder in toluene (20 mL) was added solid [1,3-$(SiMe_3)_2C_3H_3$]K (0.449 g, 2.0 mmol). The reaction mixture was stirred for 8 h at room temperature. The resulting bright orange solution was filtered and volatiles were removed *in vacuo*. The residue was redissolved in hexane (2 × 15 mL), filtered again, and dried *in vacuo* to give an orange crystalline powder (0.76 g, 70%). Suitable crystals for X-ray diffraction were grown from a concentrated hexane solution. ^{1}H NMR (C_6D_6, 500 MHz, 25 °C): δ 7.59−7.27 (m, 4H, Ind), 7.00 (t, J_{H-H} = 16.1, 1H, allyl), 6.90−6.82 (m, 4H, Ind), 6.77−6.74 (m, 1H, Ind), 6.53 (s, 1H, Ind), 6.44 (s, 1H, Ind), 6.18 (s, 1H, Ind), 3.85 (d, J_{H-H} = 16.2, 1H,

allyl), 2.25 (s, 3H, CH_3), 2.13 (s, 3H, CH_3), 1.19 (dd, J_{H-H} = 15.9 and 3.6, 1H, allyl), 0.19 (s, 9H, $SiMe_3$), −0.03 (s, 9H, $SiMe_3$). $^{13}C\{^1H\}$ NMR (C_6D_6, 125 MHz, 25 °C): δ 161.5 ($SiMe_3CHCHCHSiMe_3$), 128.1 (Ind), 123.7 (Ind), 122.8 (Ind), 120.6 (Ind), 114.6 (Ind), 113.2 (Ind), 111.2 (Ind), 101.12 (Ind), 98.6 (Ind), 91.0 ($SiMe_3CHCHCHSiMe_3$), 89.0 ($SiMe_3CHCHCHSiMe_3$), 41.1 ($C(CH_3)_2$), 28.7 ($C(CH_3)_2$), 27.9 ($C(CH_3)_2$), 0.7 ($SiMe_3$), 0.3 ($SiMe_3$). Anal. Calcd (%) for $C_{30}H_{39}Si_2Y$ (544.70): C, 66.15; H, 7.22. Found: C, 62.8; H, 7.20.[25]

***rac*-{$CMe_2(Ind)_2$}Nd(1,3-$(SiMe_3)_2C_3H_3$) (4).** Complex **4** was prepared using a similar procedure as that described above for **3**, starting from {$CMe_2(Ind)_2$}H_2 (0.546 g, 2.0 mmol), $NdCl_3(THF)_2$ (0.79 g, 2.0 mmol), and [1,3-$(SiMe_3)_2C_3H_3$]K (0.449 g, 2.0 mmol), and isolated as a brown powder (0.675 g, 56%). Because of the strong paramagnetism of Nd, ^1H NMR spectra of this compound featured only very broad, uninformative resonances. Anal. Calcd (%) for $C_{30}H_{39}NdSi_2$ (600.05): C, 60.05; H, 6.55. Found: C, 56.8; H, 7.25.[23]

Typical Procedure for Styrene Polymerization with Compounds 1−4. In the glovebox, a preweighted amount of allyl *ansa*-lanthanidocene complex (10 to 60 mg) was added to styrene (1 to 20 mL) in a Schlenk flask. The flask was then closed and immerged in an oil bath preheated at the desired temperature. Vigorous magnetic stirring was immediately started. After a given time period, the flask was opened to air and a 10% solution of HCl in methanol (*ca.* 1 mL) was added to quench the reaction. The polymer precipitated was washed repeatedly with methanol (*ca.* 500 mL), filtered and dried *in vacuo*.

Typical Procedure for Styrene Polymerization with the Binary System 1/Mg(*n*Bu)$_2$. A 30 mL Schlenk flask equipped with a magnetic bar was charged sequentially, at room temperature, with compound **1** (20 mg, 35 μmol), heptane (5 mL) and styrene (8.0 mL). The flask was immerged into an oil bath preheated at 80 °C and, and then Mg(nBu)$_2$ (0.35 mL of a 1.0 M solution in hexanes) was immediately added to the solution. After 1 h, the polymerization was quenched by adding 2 mL of acidified methanol or, for the deuterium labeling experiment, 2 mL of a 1:1 (v/v) CF_3CO_2D/CH_3OD solution; the mixture was then poured into acidified methanol. The polymers were recovered by filtration and dried at 45 °C in a vacuum oven overnight.

Computational Details. Calculations were carried out at the DFT level of theory using the hybrid functional B3PW91.[26] Geometry optimizations were carried out without any symmetry restrictions; the nature of the *extrema* (*minima* and transition states) was verified with analytical frequency calculations. Connectivity of each transition state was determined while following their intrinsic reaction coordinates (IRC). All the computations were performed with the Gaussian 03 suite of programs.[27] Yttrium was represented with a Stuttgart−Dresden pseudopotential in combination with its adapted basis set.[28] The basis set has been augmented by *f* function (α = 1.0). Carbon and hydrogen atoms have been described with all electrons 6-31G(*d*,*p*) double-ζ quality basis sets.[29]

■ ASSOCIATED CONTENT

Supporting Information. Representative GPC traces, additional NMR data and DSC analysis of iPS samples, and Cartesian coordinates of all optimized complexes. This material is available free of charge via the Internet at http://pubs.acs.org.

■ AUTHOR INFORMATION

Corresponding Author

*E-mail: jean-francois.carpentier@univ-rennes1.fr.

■ ACKNOWLEDGMENT

This work was gratefully supported by Total Petrochemicals (grants to L.A., A.-S.R. and Y.S.). J.-F.C. and L.M. thank the *Institut Universitaire de France* for Junior IUF fellowships.

■ REFERENCES

(1) (a) Rodrigues, A.-S.; Kirillov, E.; Carpentier, J.-F. *Coord. Chem. Rev.* **2008**, *252*, 2115. (b) Schellenberg, J. *Prog. Polym. Sci.* **2009**, *34*, 688.

(2) (a) Ishihara, N.; Kuramoto, M.; Uoi, M. (to Idemitsu Kosan Co. Ltd.) *Jap. Pat.* 62187708, 1985; (b) Ishihara, N.; Seimiya, T.; Kuramoto, M.; Uoi, M. *Macromolecules* **1986**, *19*, 2464.

(3) See for instance:Britovsek, G. J. P.; Gibson, V. C.; Wass, D. F. *Angew. Chem., Int. Ed.* **1999**, *38*, 428.

(4) (a) Flores, J. C.; Chien, J. C. W.; Rausch, M. D. *Organometallics* **1995**, *14*, 1927. (b) Flores, J. C.; Chien, J. C. W.; Rausch, M. D. *Organometallics* **1995**, *14*, 2106.

(5) (a) Liguori, D.; Grisi, F.; Sessa, I.; Zambelli, A. *Macromol. Chem. Phys.* **2003**, *204*, 164. (b) Liguori, D.; Centore, R.; Tuzi, A.; Grisi, F.; Sessa, I.; Zambelli, A. *Macromolecules* **2003**, *36*, 5451.

(6) (a) Capacchione, C.; Proto, A.; Ebeling, H.; Mülhaupt, R.; Moller, K.; Spaniol, T. P.; Okuda, J. *J. Am. Chem. Soc.* **2003**, *125*, 4964. (b) Capacchione, C.; Manivannan, R.; Barone, M.; Beckerle, K.; Centore, R.; Oliva, L.; Proto, A.; Tuzi, A.; Spaniol, T. P.; Okuda, J. *Organometallics* **2005**, *24*, 2971. (c) Beckerle, K.; Manivannan, R.; Lian, B.; Meppelder, G.-J. M.; Raabe, G.; Spaniol, T. P.; Ebeling, H.; Pelascini, F.; Mülhaupt, R.; Okuda, J. *Angew. Chem., Int. Ed.* **2007**, *46*, 4790. (d) Carpentier, J.-F. *Angew. Chem., Int. Ed.* **2007**, *46*, 6404. (e) Meppelder, G. J. M.; Beckerle, K.; Manivannan, R.; Lian, B.; Raabe, G.; Spaniol, T. P.; Okuda, J. *Chem.—Asian J.* **2008**, *3*, 1312.

(7) (a) Kim, Y.; Hong, E.; Lee, M. H.; Kim, J.; Han, Y.; Do, Y. *Organometallics* **1999**, *18*, 36. (b) Kim, Y.; Han, Y.; Hwang, J.-W.; Kim, M. W.; Do, Y. *Organometallics* **2002**, *21*, 1127.

(8) Harder, S. *Angew. Chem., Int. Ed.* **2004**, *43*, 2714.

(9) (a) Luo, Y.; Baldamus, J.; Hou, Z. *J. Am. Chem. Soc.* **2004**, *126*, 13910. (b) Hitzbleck, J.; Beckerle, K.; Okuda, J.; Halbach, T.; Mülhaupt, R. *Macromol. Symp.* **2006**, *236*, 23. (c) Jaroschik, F.; Shima, T.; Li, X.; Mori, K.; Ricard, L.; Le Goff, X.-F.; Nief, F.; Hou, Z. *Organometallics* **2007**, *26*, 5654. (d) Fang, X.; Li, X.; Hou, Z.; Assoud, J.; Zhao, R. *Organometallics* **2009**, *28*, 517. (e) Bonnet, F.; Da Costa Violante, C.; Roussel, P.; Mortreux, A.; Visseaux, M. *Chem. Commun.* **2009**, 3380.

(10) Zinck, P.; Valente, A.; Mortreux, A.; Visseaux, M. *Polymer* **2007**, *48*, 4609.

(11) (a) Kirillov, E.; Lehmann, C. W.; Razavi, A.; Carpentier, J.-F. *J. Am. Chem. Soc.* **2004**, *126*, 12240. (b) Rodrigues, A.-S.; Kirillov, E.; Lehmann, C. W.; Roisnel, T.; Vuillemin, B.; Razavi, A.; Carpentier, J.-F. *Chem.—Eur. J.* **2007**, *13*, 5548. (c) Perrin, L.; Sarazin, Y.; Kirillov, E.; Carpentier, J.-F.; Maron, L. *Chem.—Eur. J.* **2009**, *15*, 2773.

(12) (a) Natta, G.; Pino, P.; Corradini, P.; Danusso, F.; Mantica, E.; Mazzanti, G.; Moraglio, G. *J. Am. Chem. Soc.* **1955**, *77*, 1708. (b) Natta, G.; Corradini, P. *Makromol. Chem.* **1955**, *16*, 77. (c) Overberger, C.; Mark, H. *J. Polym. Sci.* **1959**, *35*, 381. (d) Kern, R. J.; Hurst, H. G.; Richard, W. J. *J. Polym. Sci.* **1960**, *45*, 195. For recent works, see: (e) Rosário Riberio, M.; Portela, M. F.; Deffieux, A.; Cramail, H.; Rocha, M. F. *Macromol. Rapid Commun.* **1996**, *17*, 461–469. (f) Sun, Q.; Fan, Y.; Liao, S.; Liu, J.; Wan, F.; Xu, J. *Polymer* **2001**, *42*, 4087. (g) Xu, G.; Lin, S. *Macromol. Rapid Commun.* **1994**, *15*, 873.

(13) (a) Kern, R. J. *Nature* **1960**, *187*, 410. (b) Cazzaniga, L.; Cohen, R. E. *Macromolecules* **1989**, *22*, 4125. (c) Makino, T.; Hogen-Esch, T. E. *Macromolecules* **1999**, *32*, 5712. (d) Maréchal, J.-M.; Carlotti, S.; Shcheglova, L.; Deffieux, A. *Polymer* **2004**, *45*, 4641.

(14) Nickel-catalyzed styrene polymerization:(a) Ascenso, J. R.; Dias, A. R.; Gomes, P. T.; Romao, C. C.; Tkatchenko, I.; Revillon, A.; Pham, Q. T. *Macromolecules* **1996**, *29*, 4172. (b) Crossetti, G. L.; Bormioli, C.; Ripa, A.; Giarrusso, A.; Porri, L. *Macromol. Rapid Commun.* **1997**, *18*, 801. (c) Dias, M. L.; Crossetti, G. L.; Bormioli, C.; Giarusso, A.; de Santa Maria, L. C.; Coutinho, F. M. B.; Porri, L. *Polym. Bull.* **1998**, *40*, 689. (d) Po, R.; Cardi, N.; Santi, R.; Romano, A. M.; Zannoni, C.; Spera, S. *J. Polym. Sci., Part A: Polym. Chem.* **1998**, *36*, 2119. Lanthanide-catalyzed styrene polymerization: (e) Liu, L.; Gong, Z.; Zheng, Y.; Jing, X. *J. Polym. Sci.: A: Polym. Chem.* **1998**, *36*, 1773. (f) Baudry-Barbier, D.; Camus, E.; Dormond, A.; Visseaux, M. *Appl. Organomet. Chem.* **1999**, *13*, 813.

(15) Arai, T.; Ohtsu, T.; Suzuki, S. *Polym. Prepr.* **1998**, *39*, 220–221.
(16) Preliminary communication: Rodrigues, A.-S.; Kirillov, E.; Roisnel, T.; Razavi, A.; Vuillemin, B.; Carpentier, J.-F. *Angew. Chem., Int. Ed.* **2007**, *46*, 7240.
(17) For a recent review, see:(a) Kempe, R. *Chem.—Eur. J.* **2007**, *13*, 2764; (b) Pelletier, J.-F.; Mortreux, A.; Olonde, X.; Bujadoux, K. *Angew. Chem.* **1996**, *108*, 1980; *Angew. Chem., Int. Ed. Engl.* **1996**, *35*, 1854; (c) Chenal, T.; Olonde, X.; Pelletier, J. F.; Bujadoux, K.; Mortreux, A. *Polymer* **2007**, *48*, 1844; (d) Britovsek, G. J. P.; Cohen, S. A.; Gibson, V. C.; Maddox, P. J.; van Meurs, M. *Angew. Chem.* **2002**, *114*, 507; *Angew. Chem., Int. Ed.* **2002**, *41*, 489; (e) van Meurs, M.; Britovsek, G. J. P.; Gibson, V. C.; Cohen, S. A. *J. Am. Chem. Soc.* **2005**, *127*, 9913; (f) Rogers, J. S.; Bazan, G. C. *Chem. Commun.* **2000**, 1209; (g) Kretschmer, W. P.; Meetsma, A.; Hessen, B.; Schmalz, T.; Qayyum, S.; Kempe, R. *Chem.—Eur. J.* **2006**, *12*, 8969; (h) Boisson, C.; Monteil, V.; Ribour, D.; Spitz, R.; Barbotin, F. *Macromol. Chem. Phys.* **2003**, *204*, 1747; (i) Briquel, R.; Mazzolini, J.; Le Bris, T.; Boyron, O.; Boisson, F.; Delolme, F.; D'Agosto, F.; Boisson, C.; Spitz, R. *Angew. Chem., Int. Ed.* **2008**, *47*, 1; (j) Wei, J.; Zhang, W.; Sita, L. R. *Angew. Chem.* **2010**, *122*, 1812; *Angew. Chem., Int. Ed.* **2010**, *49*, 1768.
(18) For the application of CCTP to styrene polymerization, see:(a) Bogaert, S.; Carpentier, J.-F.; Chenal, T.; Mortreux, A.; Ricart, G. *Macromol. Chem. Phys.* **2000**, *201*, 1813. (b) Sarazin, Y.; Chenal, T.; Mortreux, A.; Vezin, H.; Carpentier, J.-F. *J. Mol. Catal. A* **2005**, *238*, 207. (c) Rodrigues, A.; Kirillov, E.; Vuillemin, B.; Razavi, A.; Carpentier, J.-F. *J. Mol. Catal. A* **2007**, *273*, 87. (d) Zinck, P.; Bonnet, F.; Mortreux, A.; Visseaux, M. *Prog. Polym. Sci.* **2009**, *34*, 369. (e) Zinck, P.; Valente, A.; Bonnet, F.; Violante, A.; Mortreux, A.; Visseaux, M.; Ilinca, S.; Duchateau, R.; Roussel, P. *J. Polym. Sci., Polym. Chem.* **2010**, *48*, 802. (f) see also ref.[10]
(19) Arai, T.; Ohtsu, T.; Suzuki, S. *Macromol. Rapid Commun.* **1998**, *19*, 327.
(20) (a) Harwood, H. J.; Chen, T. K.; Lin, F. T. *ACS Symp. Ser.* **1984**, *247*, 197. (b) Chen, T. K.; Harwood, H. J. *Makromol. Chem., Rapid Commun.* **1983**, *4*, 463. (c) Kawamura, T.; Toshima, N.; Matsuzaki, K. *Macromol. Rapid Commun.* **1994**, *15*, 479. (d) Longo, P.; Grassi, A.; Oliva, L.; Ammendola, P. *Makromol. Chem.* **1990**, *191*, 237.
(21) (a) Lian, B.; Beckerle, K.; Spaniol, T. P.; Okuda, J. To be published. (b) Hohberger, C. Doctoral Dissertation, RWTH Aachen University: 2010.
(22) In contrast, the more configurationally rigid *trans*-cyclohexane-diyl-bridged catalysts $[Ti(cydtbp)(CH_3)_2]/B(C_6F_5)_3$ [cydtbp = $\{OC_6H_2$-*t*Bu_2-4,6$)_2(SC_6H_{10}S)\}$] gave iPS in which only resonance **A** was observed, i.e., *mmmmmm* > 0.99). See ref.[6]
(23) The chemical shift of resonance **C** at δ 146.26 ppm would correspond, according to earlier literature data,[20] to either a *mmmmrm* or *rmmmmr* heptad (δ 146.13 and 146.25 ppm, respectively). However, both possibilities appear to be inconsistent with the experimental data. In the first case (*mmmmrm*), resonance **C** should be accompanied by another resonance of equal intensity for the *mmmrmm* heptad, which is anticipated at δ 145.67 ppm,[20a−d] but was never observed whatever the catalyst used (Figure 9).[21] Similar considerations hold for the second possibility (*rmmmmr*), despite the much better match between, on one hand, the chemical shift observed in iPS produced with the current catalyst systems and with the Ti-{OSSO} catalysts and, on the other hand, that reported in the literature.
(24) Woodman, T. J.; Schormann, M.; Bochmann, M. *Isr. J. Chem.* **2002**, *42*, 283.
(25) Low carbon values were repetitively obtained. This problem was ascribed to the presence of silicon that is known to form non-combustible SiC. Similar difficulty in obtaining satisfactory elemental analyses for silicon-bearing complexes of group 3 metals have been encountered by many other workers; see for instance:(a) Arredondo, V. M.; Tian, S.; McDonald, F. E.; Marks, T. J. *J. Am. Chem. Soc.* **1999**, *121*, 3633. (b) Douglass, M. R.; Stern, C. L.; Marks, T. J. *J. Am. Chem. Soc.* **2001**, *123*, 10221. (c) Mitchell, P.; Hajela, S.; Brookhart, S. K.; Hardcastle, K. I.; Henling, L. M.; Bercaw, J. E. *J. Am. Chem. Soc.* **1996**, *118*, 1045.
(26) (a) Becke, A. D. *J. Chem. Phys.* **1993**, *98*, 5648. (b) Burke, K.; Perdew, J. P.; Yang, W. *Electronic Density Functional Theory: Recent Progress and New Directions*; Dobson, J. F., Vignale, G., Das, M. P. Eds.; Plenum Press: New York, 1998 .
(27) Frisch, M. J.; Trucks, G. W.; Schlegel, H. B.; Scuseria, G. E.; Robb, M. A.; Cheeseman, J. R.; Zakrzewski, V. G.; Montgomery, J. A.; Stratman, R. E.; Burant, J. C.; Dapprich, S.; Millam, J. M.; Daniels, A. D.; Kudin, K. N.; Strain, M. C.; Farkas, O.; Tomasi, J.; Barone, V.; Cossi, M.; Cammi, R.; Mennucci, B.; Pomelli, C.; Adamo, C.; Clifford, S.; Ochterski, J.; Petersson, G. A.; Ayala, P. Y.; Cui, Q.; Morokuma, K.; Malick, D. K.; Rabuck, A. D.; Raghavachari, K.; Foresman, J. B.; Cioslowswi, J.; Ortiz, J. V.; Baboul, A. G.; Stefanov, B. B.; Liu, G.; Liashenko, A.; Piskorz, P.; Komaromi, I.; Gomperts, R.; Martin, R.; Fox, D. J.; Keith, T.; Al-Laham, M. A.; Peng, C. Y.; Nanayakkara, A.; Gonzalez, C.; Challacombe, M.; Gill, P. M. W.; Jonhson, B.; Chen, W.; Wong, M. W.; Andres, J. L.; Head-Gordon, M.; Replogle, E. S.; Pople, J. A. *Gaussian 03, Revision D-02*; Gaussian, Inc.: Pittsburgh, PA, 2003.
(28) Andrae, D.; Haeussermann, U.; Dolg, M.; Stoll, H.; Preuss, H. *Theor. Chim. Acta* **1990**, *77*, 123.
(29) Hariharan, P. C.; Pople, J. A. *Theor. Chim. Acta* **1973**, *28*, 213.